



Deposited via The University of Leeds.

White Rose Research Online URL for this paper:

<https://eprints.whiterose.ac.uk/id/eprint/168111/>

Version: Accepted Version

Article:

Liu, K, Wei, Z, Yang, Z et al. (2021) Mass load prediction for lithium-ion battery electrode clean production: a machine learning approach. *Journal of Cleaner Production*, 289. 125159. ISSN: 0959-6526

<https://doi.org/10.1016/j.jclepro.2020.125159>

© 2020 Elsevier Ltd. Licensed under the Creative Commons Attribution-NonCommercial-NoDerivatives 4.0 International License (<http://creativecommons.org/licenses/by-nc-nd/4.0/>).

Reuse

This article is distributed under the terms of the Creative Commons Attribution-NonCommercial-NoDerivs (CC BY-NC-ND) licence. This licence only allows you to download this work and share it with others as long as you credit the authors, but you can't change the article in any way or use it commercially. More information and the full terms of the licence here: <https://creativecommons.org/licenses/>

Takedown

If you consider content in White Rose Research Online to be in breach of UK law, please notify us by emailing eprints@whiterose.ac.uk including the URL of the record and the reason for the withdrawal request.

1 Mass load prediction for lithium-ion battery electrode clean 2 production: a machine learning approach

3 Kailong Liu^{a*}, Zhongbao Wei^b, Zhile Yang^c, Kang Li^{d*}

4 *a* WMG, The University of Warwick, Coventry, CV4 7AL, United Kingdom {Email: kliu02@qub.ac.uk,
5 kailong.liu@warwick.ac.uk}.

6 *b* National Engineering Laboratory for Electric Vehicles, School of Mechanical Engineering, Beijing Institute of
7 Technology, Beijing 100081, China {Email: weizb@bit.edu.cn}.

8 *c* Shenzhen Institute of Advanced Technology, Chinese Academy of Sciences, Shenzhen, Guangdong, 518055,
9 China {Email: zl.yang@siat.ac.cn}.

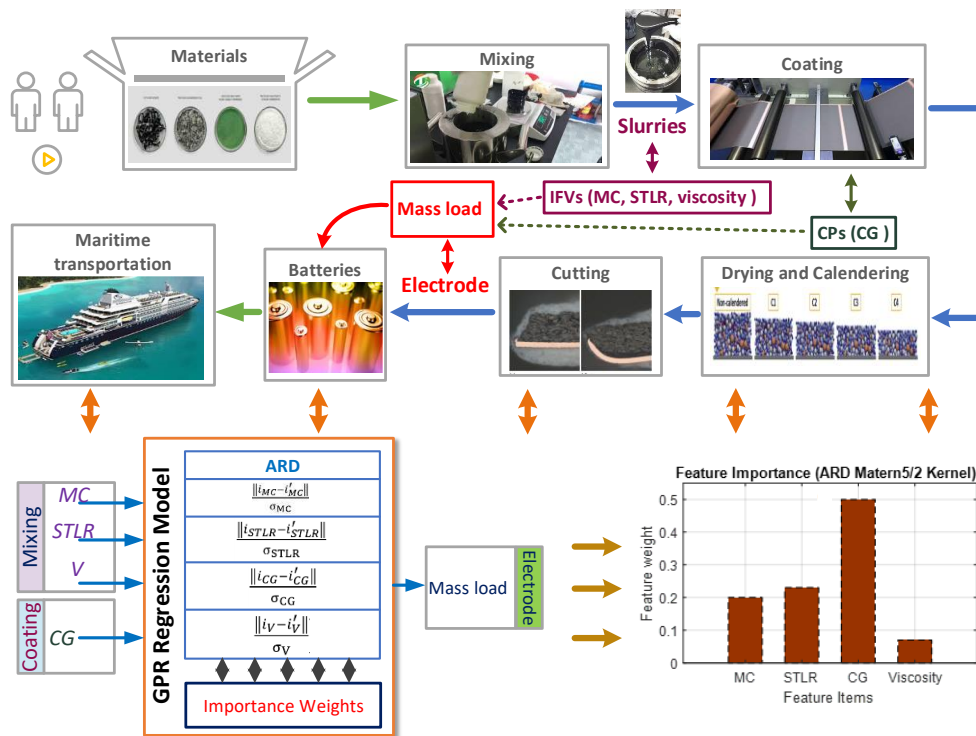
10 *d* School of Electronic and Electric Engineering, University of Leeds, LS2 9JT, United Kingdom {Email:
11 k.li1@leeds.ac.uk}

12 * Corresponding author
13

14 **Abstract:** With the advent of sustainable and clean energy, lithium-ion batteries have been widely utilised in
15 cleaner productions such as energy storage systems and electrical vehicles, but the management of their electrode
16 production chain has a direct and crucial impact on the battery performance and production efficiency. To achieve
17 a cleaner production chain of battery electrode involving strongly-coupled intermediate parameters and control
18 parameters, a reliable approach to quantify the feature importance and select the key feature variables for
19 predicting battery intermediate products is urgently required. In this paper, a Gaussian process regression-based
20 machine learning framework, which incorporates powerful automatic relevance determination kernels, is
21 proposed for directly quantifying the importance of four intermediate production feature variables and analysing
22 their influences on the prediction of battery electrode mass load. Specifically, these features include three
23 intermediate parameters from the mixing step and a control parameter from the coating step. After deriving four
24 different automatic relevance determination kernels, the importance of these four feature variables based on a
25 regression modelling is comprehensively analysed. Comparative results demonstrate that the proposed automatic
26 relevance determination kernel-based Gaussian process regression models could not only quantify the importance
27 weights for reliable feature selections but also help to achieve satisfactory electrode mass load prediction. Due to
28 the data-driven nature, the proposed framework can be conveniently extended to improve the analysis and control
29 of battery electrode production, further benefitting the manufactured battery yield, efficiencies and performance
30 to achieve cleaner battery production.

1 **Key words:** Battery electrode production; data-driven model; mass load prediction; efficient energy storage
 2 system; cleaner production.

3 **Graphical Abstract:**



4

5 **A list of terminology and symbols**

6	Li-ion	lithium-ion
7	EV	electrical vehicle
8	CRISP	cross-industry standard process
9	IFV	intermediate feature variable
10	CP	control parameter
11	GPR	Gaussian process regression
12	ARD	automatic relevance determination
13	EX	exponential
14	SE	squared-exponential
15	NMP	N-Methyl-2-pyrrolidone
16	PVDF	polyvinylidene difluoride
17	MC	mass content
18	STLR	solid-to-liquid ratio
19	CG	comma gap
20	MAE	mean absolute error
21	RMSE	root mean square error
22	$m(j)$	mean function
23	$k(j, j')$	covariance function
24	θ_{hp}	hyper-parameters
25	$L(\theta_{hp})$	negative log marginal likelihood
26	$p(y' j, y, j')$	conditional distributions

1	\bar{y}'	mean prediction value
2	\mathbf{N}	distribution matrix
3	\mathbf{cov}	variance matrix
4	k_{EX}	exponential kernel
5	k_{SE}	squared-exponential kernel
6	$k_{M3/2}$	Matern3/2 kernel
7	$k_{M5/2}$	Matern5/2 kernel
8	k_{ARDEX}	exponential kernel with ARD structure
9	k_{ARDSE}	squared-exponential kernel with ARD structure
10	$k_{ARDM3/2}$	Matern3/2 kernel with ARD structure
11	$k_{ARDM5/2}$	Matern5/2 kernel with ARD structure
12	W	feature weights
13		

14 1. Introduction

15 Nowadays, lithium-ion (Li-ion) batteries have been widely utilised to boost the development of cleaner
 16 productions such as electrical vehicles (EVs) and energy storage systems, due to their low discharge-rates and
 17 high energy densities (Liu, C. et al., 2019). However, the performance of Li-ion batteries would be directly and
 18 highly affected by their electrode production processes, which significantly hinders the improvements of battery
 19 technology. The battery electrode production is of great concern in developing clean and effective energy storage
 20 systems, which is a key factor in securing tangible economic payback and in improving the efficiencies of large-
 21 scale clean energy applications (Dahodwalla and Herat, 2000). In light of this, efforts are urgently needed to fully
 22 understand the intermediate products and parameters within the battery electrode production chain (He et al.,
 23 2020).

24 Unfortunately, battery electrode production chain contains numerous intermediate processes with a large amount
 25 of intermediate products, parameters and influencing factors (Lee et al., 2010). Due to the complexity and strong-
 26 coupled interdependencies of electrode manufacturing steps, the multiple correlations among feature variables of
 27 intermediate products and control parameters are still difficult to model. As the whole battery production chain
 28 consists of a number of chemical, mechanical as well as electrical operations and would generate over 600
 29 influencing parameters or variables, the analysis of feature variables in electrode production requires the deep
 30 expert experiences and specialized equipment, which still mainly relies on the trial and error solutions (Kwade et
 31 al., 2018; Pang et al., 2019). Therefore, in order to achieve smarter and cleaner battery production, advanced data
 32 analysis strategies to better quantify feature variables and select key feature items for predicting battery electrode
 33 properties are urgently needed.

1 With the rapid development of artificial intelligence and machine learning technologies, data-driven strategies
2 have become popular in the field of battery management (Li et al., 2019; Lipu et al., 2018; Zhou et al., 2020). A
3 range of data-driven approaches have been designed for estimating battery states (Meng et al., 2019; Tian et al.,
4 2020; Wei et al., 2019; Zhou et al., 2019), predicting battery lifetime during cycling (Tang et al., 2019; Zhang et
5 al., 2019) or storage modes (Liu et al., 2019), diagnosing battery faults (Pan et al., 2020; Yang, R. et al., 2018),
6 balancing battery cells (Ouyang et al., 2020; Saw et al., 2016), achieving efficient thermal management (Shang et
7 al., 2019; Xiong et al., 2018) and charging management (Liu et al., 2018; Maia et al., 2019). Overall, through
8 designing suitable data-driven models, it is expected that smarter and more efficient management of Li-ion
9 batteries can be achieved. However, these researches primarily focus on the battery macroscopic performance
10 without taking the battery intermediate properties in the production process into account. It should be noted that
11 the battery production chain also generates a large amount of data and plays a more direct role in determining the
12 battery performance, designing an effective data-driven approach to quantify and predict battery intermediate
13 features is therefore also crucial for boosting the development of cleaner production (Dahodwalla and Herat, 2000).

14 In contrast to the battery management where fruitful solutions are available, less reports have been found so far
15 on using advanced machine learning technologies to improve the battery production (Wanner et al., 2019). Among
16 limited literatures on battery productions (e.g. monitoring (Knoche et al., 2016), adjustment (Schünemann et al.,
17 2016) and control (Günther et al., 2020)), developing a proper data-driven based model to analyse feature variables
18 and predict intermediate product properties is a hotspot. For instance, a data-driven approach was proposed in
19 (Schnell and Reinhart, 2016) to analyse the failure modes and parametric effects, which contributes to the
20 improvement of battery production chain control. Based on the cross-industry standard process (CRISP), Schnell
21 et al. (Schnell et al., 2019) designed a linear model and a neural network model to identify the process
22 dependencies and forecast the battery production properties. Turetskyy et al. (Turetskyy et al., 2019) utilised the
23 decision tree techniques to analyse feature importance and forecast the maximum capacity of battery. A multi-
24 variate data-driven model was designed in (Thiede et al., 2019) to discover proper quality gates for predicting the
25 manufactured battery properties. Based upon the statistical analyses of fluctuations in battery production, the
26 influence of these fluctuations on manufactured battery capacity is evaluated in (Hoffmann et al., 2019). In (Cunha
27 et al., 2020), several 2D graphs produced by three conventional machine learning classification models are used
28 to analyse the dependencies of battery production features. Despite the aforementioned works on the data-driven

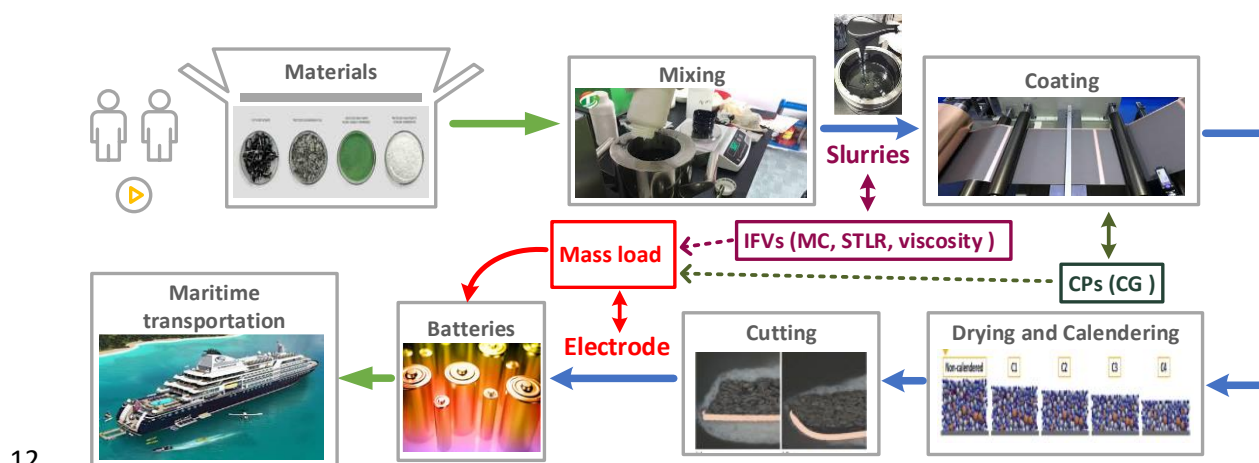
1 modelling of battery production, several limitations and challenges remain to be improved: 1) most researches
2 simply apply conventional methodologies to predict the properties of battery production, little has been done to
3 comprehensively evaluate the data-driven approaches to further improve their performance in battery production
4 area. 2) commonly-used machine learning technologies such as support vector machines and neural networks only
5 produce predictions of battery production properties, but fail to directly quantify the importance of battery
6 production features which is also of interests to engineers. Such information could benefit engineers to conduct
7 sensitivity analysis for effective feature selection and optimise the production chain to further enhance the
8 manufactured batteries performance and achieve cleaner battery production.

9 Given the aforementioned considerations, this article deals with the data-driven electrode property prediction for
10 Li-ion battery production, where the importance weights of multiple battery production feature items can be also
11 taken into account. The main contributions of this paper are summarized as follows: 1) After identifying four
12 feature items of interest from three intermediate feature variables (IFVs) in the mixing step and a control parameter
13 (CP) in the coating step of the battery production process, a Gaussian process regression (GPR)-based machine
14 learning framework is designed to effectively map the underlying relations among these feature items and the
15 battery electrode mass load. 2) The kernel functions within GPR are enhanced with an automatic relevance
16 determination (ARD) structure, allowing multiple input variables to obtain different scales of hyper-parameters
17 to improve the regression accuracy and robustness. 3) Based upon the well-tuned hyper-parameters within the
18 ARD kernels, the importance weights of these feature variables of interest could be effectively quantified for the
19 reliable selections of battery production features. 4) The importance of these feature items and the prediction
20 results are comprehensively evaluated and quantified with four different ARD kernels derived from the
21 exponential (EX), squared-exponential (SE), Matern3/2 and Matern5/2 covariance functions. This is the first
22 known application by designing the ARD kernel-based GPR to directly and simultaneously quantify the weights
23 of battery feature items and analyse their effects on the regressions of battery electrode mass load. Obviously, the
24 proposed ARD kernel-based GPR framework could bring the significant benefits such as better monitoring the
25 key variables within battery production chain to enhance the manufactured battery yield, efficiencies and
26 performance, as well as saving the costs of battery production, further leading to cleaner battery production and
27 improving the optimisation of energy storage system.

1 The remainder of this paper is organized as follows. Section 2 describes some key steps and variables within the
 2 battery electrode production chain. Section 3 presents the fundamental of GPR, ARD kernels, detailed feature
 3 selection workflow and several performance indicators. Section 4 gives an in-depth comparison of the prediction
 4 results of electrode mass load and discuss the quantified importance weights of all features of interest. Finally,
 5 Section 5 concludes this paper.

6 2. Battery electrode production chain

7 Electrode production is a primary and significantly sophisticated process in the battery manufacturing chain,
 8 covering multiple disciplines such as mechanical engineering, chemical engineering and electrical engineering
 9 (Chouchane et al., 2019). Moreover, the properties of manufactured electrode such as mass load plays a key role
 10 in determining the battery final performance (energy or power densities, maximal capacity and service life), which
 11 must be carefully managed for benefitting the cleaner battery production.



12 **Fig. 1.** A systematic framework of some key steps in battery electrode production chain.

14 Fig. 1 gives a systematic framework illustrating some key steps in the battery electrode production chain. It should
 15 be known that battery electrode manufacturing is a lengthy process involving many intermediate and individual
 16 steps (i.e., mixing, coating, drying, calendaring and cutting) as well as specialized equipment (i.e., mixer, coater,
 17 oven). In this framework, the first key process is the mixing step which produces the slurries for both anodes and
 18 cathodes. Specifically, in the mixing step, the prepared active materials such as graphite and Li-NCM-Oxide, the
 19 conductive additive material such as carbon black, the solvent such as N-Methyl-2-pyrrolidone (NMP) as well as
 20 the binder such as polyvinylidene difluoride (PVDF) will be mixed within a soft blender. A standard process is

1 that the binder is first dissolved into the solvent, followed by adding the active and conductive additive materials
2 to produce slurries. After mixing, these mixed slurries would be coated upon both two surface sides of metal
3 foils by a comma-gap coater. In general, the copper foil is utilised for anode coating while the aluminium foil is
4 adopted for cathode coating. In this stage, the speed of coater would be fixed and the comma gap is changed to
5 ensure shear force for determining the coating thickness. Moreover, the wet coating products will be dried by
6 setting constant temperatures of several built-in ovens simultaneously. Then, a calendaring step will follow to
7 evaporate the residual solvent of dried coating products. Finally, both anode and cathode electrodes are obtained
8 after cutting the coating products into proper sizes. It should be known that numerous variables and parameters
9 are involved in such a complex production chain. Several IFVs and CPs are of extreme importance for determining
10 the properties of electrodes, which would further affect the battery production results and must be well studied
11 and controlled.

12 In this context, three key IFVs including the active material's mass content (MC), solid-to-liquid ratio (STLR)
13 and slurry viscosity from mixing process as well as one CP named coater comma gap (CG) from coating process
14 are selected as the interested feature variables. Then an ARD kernel-based GPR framework is derived to quantify
15 the weights of these four interested features and analyse their effects on the prediction performance of battery
16 electrode mass load. In theory, STLR could reflect the mass ratios among the solid components (i.e., active
17 materials, conductive additive materials as well as binder) and the mass of slurries (i.e., solvents and solid
18 components). Slurry viscosity would highly affect the coating step and is generally related to the shear rates of
19 coating. CG reflects the gap value between the comma roll and coating roll, which could impact the weight and
20 thickness of coating products. To describe battery electrode property, the mass load of uncalendered electrode
21 with the unit of mg/cm^2 is utilised because it has a direct relation with the final electrode capacity. To well analyse
22 these feature variables and select the most important features for predicting battery electrode property, the original
23 dataset from Franco Laboratoire de Reactivite et Chimie des Solides (LRCS) is used in this study. The
24 effectiveness of this dataset has been validated in (Cunha et al., 2020). More detailed information regarding the
25 experimental design and process description can be found in (Cunha et al., 2020), which would not be repeatedly
26 described here due to space limitation. According to this dataset, effective ARD-kernel based GPR models can be
27 developed for predicting the electrode mass load. The feature weights as well as regression performance of various
28 ARD kernels can be also quantified.

1 3. Technology

2 In this section, the fundamental of GPR is first introduced, followed by the descriptions of designing various ARD
3 kernels within GPR for feature weight analysis and selection. Furthermore, the performance indicators to quantify
4 and evaluate model regression performance are also provided.

5 3.1 Gaussian process regression

6 Based upon the Bayesian framework, GPR provides a random procedure to conduct non-parametric regressions
7 by the Gaussian process (Liu, K. et al., 2019; Tagade et al., 2020). For any inputs, GPR generally contains a mean
8 function $m(j)$ and a covariance function $k(j, j')$ to reflect the probability distributions as follows:

$$9 \quad f(j) \sim GPR(m(j), k(j, j')) \quad (1)$$

10 where $m(j)$ and $k(j, j')$ can be further expressed as:

$$11 \quad \begin{cases} m(j) = E(f(j)) \\ k(j, j') = E[(m(j) - f(j'))(m(j) - f(j'))] \end{cases} \quad (2)$$

12 In real applications, $m(j)$ is usually set as zero to simplify the computational effort (Liu et al., 2020). Covariance
13 function $k(j, j')$ is also called as the kernel function to reflect the correlations between the target observations of
14 training dataset and the prediction outputs by the similarities of respective input.

15 For a regression, the prior distributions of output could be defined as:

$$16 \quad y \sim \mathbf{N}(0, k(j, j')) \quad (3)$$

17 where $\mathbf{N}(\cdot)$ is a distribution matrix. Supposing both training set j and testing set j' have the same Gaussian
18 distribution, then the regression test outputs y' will provide the joint prior distributions with the training outputs
19 y as (Rasmussen and Williams, 2006):

$$20 \quad \begin{bmatrix} y \\ y' \end{bmatrix} \sim \mathbf{N}\left(0, \begin{bmatrix} k(j, j) & k(j, j') \\ k(j, j')^T & k(j', j') \end{bmatrix}\right) \quad (4)$$

21 where $k(j, j)$, $k(j', j')$ are the covariance values among inputs of training set and testing set, respectively. $k(j, j')$
22 stands for the covariance values among inputs from training and testing sets.

23 To achieve an efficient regression based on GPR model, the hyper-parameters θ_{hp} within covariance or kernel
24 function should be well tuned during training stage. A common and effective tuning way is through using gradient

1 descent or heuristic methods to minimize the negative log marginal likelihood $L(\theta_{hp})$ (Richardson et al., 2019;
2 Yang, D. et al., 2018) as:

$$3 \quad L(\theta_{hp}) = -\log p(y|\theta_{hp}) = \frac{1}{2} \log[\det k(\theta_{hp})] + \frac{1}{2} y^T k^{-1}(\theta_{hp}) y + \frac{N}{2} \log(2\pi) \quad (5)$$

4 After tuning all θ_{hp} within GPR model, the forested outputs y' related to the dataset j' could be obtained by
5 computing its corresponding conditional distributions $p(y'|j, y, j')$ by:

$$6 \quad p(y'|j, y, j') \sim \mathbf{N}(y'|\bar{y}', \mathbf{cov}(y')) \quad (6)$$

7 with

$$8 \quad \begin{cases} \bar{y}' = k(i, i')^T [k(i, i)]^{-1} y \\ \mathbf{cov}(y') = k(i', i') - k(i, i')^T [k(i, i)]^{-1} k(i, i') \end{cases} \quad (7)$$

9 where \bar{y}' reflects the mean value of predictions. $\mathbf{cov}(y')$ is a variance matrix of these predictions.

10 3.2 ARD kernel structures

11 According to the discussions in the above subsection, the kernel function within GPR must be carefully designed
12 because it significantly affects the performance of GPR. Although there exist several powerful kernels for GPR
13 in the literature, a suitable one designed for a specific application is favourable (Zhang et al., 2020). For real
14 regression applications of GPR, some typical and efficient kernels are particularly noteworthy.

15 The first one is the EX kernel with an exponential form as:

$$16 \quad k_{EX}(i, i') = \sigma_{EX}^2 \exp\left(-\frac{\|i-i'\|}{\sigma_1}\right) \quad (8)$$

17 where σ_{EX} and σ_1 are two hyper-parameters to determine the amplitude and length ranges of EX kernel. On the
18 basis of EX kernel, another popular kernel named squared-exponential (SE) kernel with two hyper-parameters
19 (σ_{SE} and σ_1) can be derived as:

$$20 \quad k_{SE}(i, i') = \sigma_{SE}^2 \exp\left(-\frac{\|i-i'\|^2}{2\sigma_1^2}\right) \quad (9)$$

21 It should be known that both EX and SE kernels belong to the fundamental type in that the correlation between
22 two various observations is purely affected by $i - i'$, which would result in the smooth distributions. This may be

1 too strict for predicting battery electrode property with highly nonlinear behaviour. To further improve the
 2 nonlinear capture capability of GPR, two powerful covariance functions named Matern3/2 kernel and Matern5/2
 3 kernel as expressed in Eq. (9) and (10) can be adopted.

$$4 \quad k_{M3/2}(i, i') = \sigma_{M3/2}^2 \left(1 + \frac{\sqrt{3}\|i-i'\|}{\sigma_1} \right) \exp\left(-\frac{\sqrt{3}\|i-i'\|}{\sigma_1}\right) \quad (10)$$

$$5 \quad k_{M5/2}(i, i') = \sigma_{M5/2}^2 \left(1 + \frac{\sqrt{5}\|i-i'\|}{\sigma_1} + \frac{5\|i-i'\|^2}{3\sigma_1^2} \right) \exp\left(-\frac{\sqrt{5}\|i-i'\|}{\sigma_1}\right) \quad (11)$$

6 where $\sigma_{M3/2}$ and $\sigma_{M5/2}$ stand for the hyper-parameters to control the amplitudes of Matern3/2 kernel and
 7 Matern5/2 kernel, respectively. σ_1 is another hyper-parameter.

8 In real applications with multiple input variables, although the EX, SE and Matern kernels have simple structure
 9 associated with a few hyper-parameters, they present limitations to fully capture the highly nonlinear relations. In
 10 our study, the inputs of interest are composed of four different IFVs (MC, STLR, CG, and viscosity). In order to
 11 well extract these input items as well as enhance the regression performance, conventional kernels including EX,
 12 SE, Matern3/2 and Matern5/2 are further reconstructed with the powerful ARD structures as ARDEX, ARDSE,
 13 ARDMatern3/2 and ARDMatern5/2 (Rasmussen and Williams, 2006), with the form of Eqs. (12), (13), (14) and
 14 (15), respectively.

$$15 \quad k_{ARDEX}(i, i') = \sigma_{EX}^2 \exp\left(-\sum_{c=1}^C \frac{\|i_c - i'_c\|}{\sigma_c}\right) \quad (12)$$

$$16 \quad k_{ARDSE}(i, i') = \sigma_{SE}^2 \exp\left(-\frac{1}{2} \sum_{c=1}^C \frac{\|i_c - i'_c\|^2}{\sigma_c^2}\right) \quad (13)$$

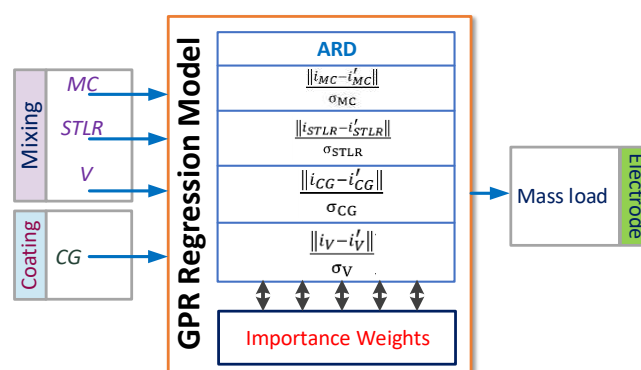
$$17 \quad \begin{cases} k_{ARDM3/2}(i, i') = \sigma_{M3/2}^2 (1 + \sqrt{3}r) \exp(-\sqrt{3}r) \\ r = \sqrt{\sum_{c=1}^C \frac{\|i_c - i'_c\|^2}{\sigma_c^2}} \end{cases} \quad (14)$$

$$18 \quad \begin{cases} k_{ARDM5/2}(i, i') = \sigma_{M5/2}^2 \left(1 + \sqrt{5}r + \frac{5}{3}r^2 \right) \exp(-\sqrt{5}r) \\ r = \sqrt{\sum_{c=1}^C \frac{\|i_c - i'_c\|^2}{\sigma_c^2}} \end{cases} \quad (15)$$

As mentioned in related research (Jacobs, 2012; Zhang et al., 2020; Zhao et al., 2019), ARD kernel can be seen as a powerful tool to conduct features extraction and improve prediction performance in many industrial applications. By using the ARD kernel for battery electrode mass load prediction, the effects of input features (MC, STLR, viscosity and CG) on the prediction can be automatically adjusted by optimising and fixing various length scales for their hyper-parameters σ_c (here $c = 1: C$, C is the total number of input items), yielding a sparse and explanatory subset of features. It should be known that for battery production applications, the effects of feature variables on the electrode mass load could not be always same. In comparison with the conventional kernels have only one length scale for all hyper-parameters, various predictors with different length scales of hyper-parameters in ARD kernels have the potential to reduce the effects of less irrelevant feature variables and improve prediction accuracy in theory. Besides, the value of σ_c could also reflect the importance and effect of related input item. A larger σ_c results in a lower relevancy which indicates a less impact on the regression output. Benefited from this, ARD kernels could be utilised as efficient tools for direct feature variable selection. Through adopting ARD kernels for battery electrode mass load predictions, the importance weights of interested features are able to be quantified as well as selected, while the regression performance and generalization could be also enhanced by setting various length-scales of σ_c . Detailed procedures of designing ARD kernels for battery intermediate product feature selection would be described in the next subsection.

3.3 ARD kernel for feature selection

As the electrode production chain is constituted of multiple intermediate processes involving numerous IFVs and CPs, establishing a data-driven model to present effective regression predictions and quantify the importance weight of feature variables is significantly attractive.



21

22 **Fig. 2.** GPR-based machine learning model to predict electrode mass load and analyse feature importance weights.

1 For the electrode production chain, the mixing and coating steps play the important roles in determining the
 2 electrode mass load, further affecting the final battery performance. In our study, to well capture the underlying
 3 correlations among feature variables and electrode mass load, a GPR-based machine learning model is designed
 4 and illustrated in Fig. 2, while the related ARD structure-based kernels would be derived as follows:

$$5 \quad k_{ARDEX}(i, i') = \sigma_{EX}^2 \exp \left[- \left(\frac{\|i_{MC} - i'_{MC}\|}{\sigma_{MC}} + \frac{\|i_{STLR} - i'_{STLR}\|}{\sigma_{STLR}} + \frac{\|i_{CG} - i'_{CG}\|}{\sigma_{CG}} + \frac{\|i_V - i'_V\|}{\sigma_V} \right) \right] \quad (16)$$

$$6 \quad k_{ARDSE}(i, i') = \sigma_{SE}^2 \exp \left[- \frac{1}{2} \left(\frac{\|i_{MC} - i'_{MC}\|^2}{\sigma_{MC}^2} + \frac{\|i_{STLR} - i'_{STLR}\|^2}{\sigma_{STLR}^2} + \frac{\|i_{CG} - i'_{CG}\|^2}{\sigma_{CG}^2} + \frac{\|i_V - i'_V\|^2}{\sigma_V^2} \right) \right] \quad (17)$$

$$7 \quad \begin{cases} k_{ARDM3/2}(i, i') = \sigma_{M3/2}^2 (1 + \sqrt{3}r) \exp(-\sqrt{3}r) \\ r = \sqrt{\frac{\|i_{MC} - i'_{MC}\|^2}{\sigma_{MC}^2} + \frac{\|i_{STLR} - i'_{STLR}\|^2}{\sigma_{STLR}^2} + \frac{\|i_{CG} - i'_{CG}\|^2}{\sigma_{CG}^2} + \frac{\|i_V - i'_V\|^2}{\sigma_V^2}} \end{cases} \quad (18)$$

$$8 \quad \begin{cases} k_{ARDM5/2}(i, i') = \sigma_{M5/2}^2 \left(1 + \sqrt{5}r + \frac{5}{3}r^2 \right) \exp(-\sqrt{5}r) \\ r = \sqrt{\frac{\|i_{MC} - i'_{MC}\|^2}{\sigma_{MC}^2} + \frac{\|i_{STLR} - i'_{STLR}\|^2}{\sigma_{STLR}^2} + \frac{\|i_{CG} - i'_{CG}\|^2}{\sigma_{CG}^2} + \frac{\|i_V - i'_V\|^2}{\sigma_V^2}} \end{cases} \quad (19)$$

9 where all ARD kernels have the same set of input items as $i = \{i_{MC}, i_{STLR}, i_{CG}, i_V\}$. σ_{MC} , σ_{STLR} , σ_{CG} , and σ_V
 10 represent the hyper-parameters to reflect the relevancies and importance of feature variables including MC, STLR,
 11 CG and viscosity, respectively. Based upon these defined ARD kernels, the detailed workflow to design GPR
 12 model for the feature selection and the regression prediction of electrode mass load is illustrated in Table 1.

13

14 **Table 1.** Detailed workflow to design the ARD kernel-based GPR for feature selection and regression of electrode mass load

1: Procedure: data pre-process and ARD kernel-based GPR training
a. Remove obvious outliers of original data
b. Prepare the proper inputs-output pairs for GPR training. Here the inputs are four intermediate feature variables while output is the related electrode mass load.
c. Optimise hyper-parameters θ_{hp} within ARD kernel-based GPR to minimize its $L(\theta_{hp})$ through four folds cross-validation. Afterwards, obtain the well-trained GPR model $GPR_{ARD}(\theta_{hp})$.
End procedure
2: Procedure: feature selections and regression of electrode mass load
a. According to the θ_{hp} , calculate the feature weights by using the equation as follows:
$W = \exp(-\theta_{hp})$ (20)

where $\theta_{hp} = \{\sigma_{MC}, \sigma_{STLR}, \sigma_{CG}, \sigma_V\}$ represent the well-tuned hyper-parameters of feature variable MC, STLR,CG and viscosity, respectively. $W = \{W_{MC}, W_{STLR}, W_{CG}, W_V\}$ are their corresponding feature weights through taking the exponential of the negative hyper-parameters.

b. Quantify the feature importance by normalizing feature weights as:

$$W = W / (W_{MC} + W_{STLR} + W_{CG} + W_V) \quad (21)$$

c. For a new sample i' from testing dataset, use the well-trained $GPR_{ARD}(\theta_{hp})$ to predict related electrode mass load y' as:

$$y' = GPR_{ARD}(i' | \theta_{hp}) \quad (22)$$

End procedure

1

2

It should be known that taking the exponential of the negative learned θ_{hp} and normalizing W is one common solution to make the quantified feature weights become more convenient for comparison purpose (Zhang et al., 2020; Zheng and Casari, 2018). Different weighting solutions such as the inverse of θ_{hp} would lead the final quantified weight values slightly change but it would not affect the ranking of features. The feature with higher ranking (larger normalized weight value) means this feature is more important than others in determining the prediction result of electrode mass load. The quantified weight values here cannot be utilised to reflect the specific contribution proportion of using these feature variables (Dong and Liu, 2018; Zheng and Casari, 2018). In light of this, all feature weights are uniformly quantified by using Eqs. (20) and (21) in our study. Following this workflow, the weights of input items including the MC, STLR, viscosity from mixing step and the CG from coating step can be directly quantified to reflect their importance. Then the reliable feature selections can be carried out based on these quantified feature weights. Besides, the designed ARD kernel-based GPR model is capable of generating an explanatory subset of features by setting different hyper-parameters for all inputted feature variables, further helping to improve the performance and generalization ability of electrode mass load regression.

16

3.4 Performance metrics

17

To investigate the performance of the designed ARD-kernel based GPRs in electrode mass load prediction, the following four performance metrics are utilised.

18

19

1) Training time: to evaluate and compare the computation efforts of different ARD kernels, the time during GPR training process is utilised. In our study, all GPR regression models are trained through using the GPR toolbox in

20

1 Matlab 2018b. The training time with the unit second (s) for GPR model can be conveniently obtained by using
2 *tic, toc* codes from the Matlab.

3 2) Mean absolute error (MAE): supposing N represents the total amount of regression samples, y_j are the actual
4 testing values while \hat{y}_j stand for the regression values from GPR, then the MAE can be obtained to evaluate the
5 accuracy of predictions as follows:

$$6 \quad \text{MAE} = \frac{1}{N} \sum_{j=1}^N |y_j - \hat{y}_j| \quad (23)$$

7 3) Root mean square error (RMSE): RMSE is another typical indicator to illustrate the deviations between the
8 regression and actual testing values as follows:

$$9 \quad \text{RMSE} = \sqrt{\frac{1}{N} \sum_{j=1}^N (y_j - \hat{y}_j)^2} \quad (24)$$

10 **4. Results and discussions**

11 To well analyse and evaluate the feature selection and regression performance of GPR with various ARD kernels,
12 two case studies including the one with all features as well as another with reduced features are carried out in this
13 section.

14 **4.1 Case study 1: all features**

15 For case study 1, to quantify the weights of interested feature variables on the regression of electrode mass load,
16 all feature items including MC, STLR, CG and viscosity are utilised as the inputs for GPR models. The regression
17 performance of all four ARD kernels are evaluated using the four-fold cross-validation. Fig. 3 and Table 2
18 illustrate the regression results and the corresponding performance metrics for the four ARD kernel-based GPRs,
19 respectively.

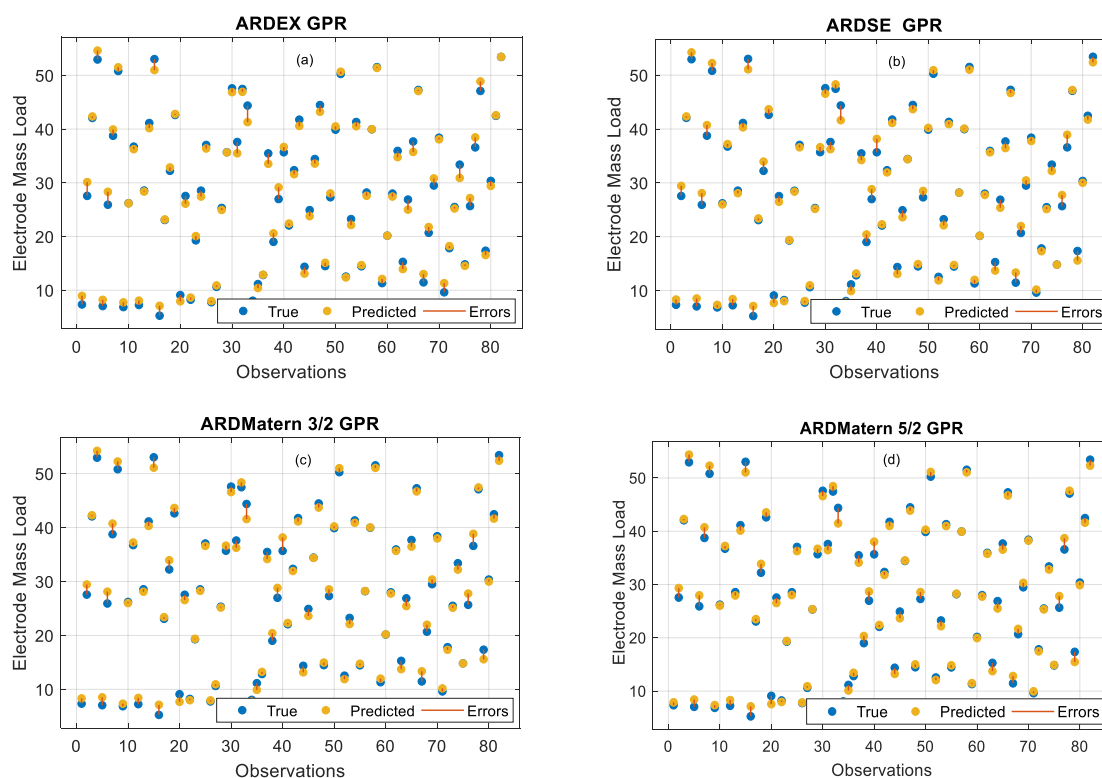


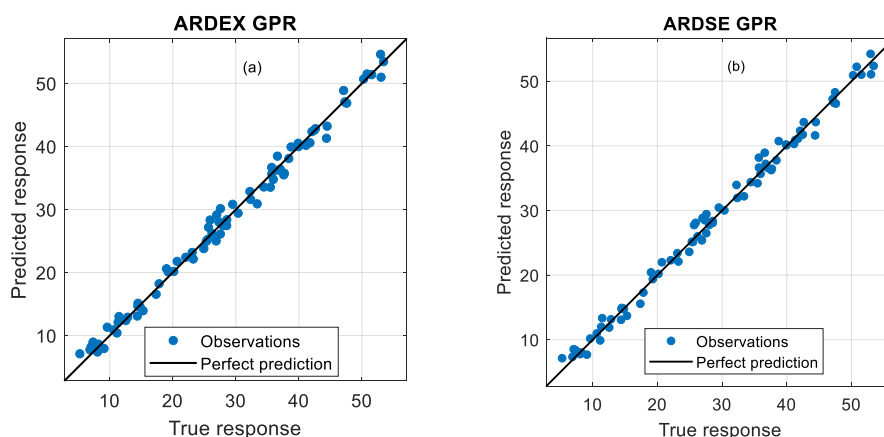
Fig. 3. Regression results through using all feature items for battery electrode mass load predictions: (a) ARDEX kernel, (b) ARDSE kernel, (c) ARDMatern3/2 kernel, (d) ARDMatern5/2 kernel.

Obviously, most observations in Fig. 3 agree well with the outputs from four GPRs, indicating that the used ARD kernels can achieve satisfactory prediction results for the electrode mass load. Quantitatively, due to the simplest structure, ARDEX kernel-based GPR can be well-trained within 13.547 s, while its accuracy is the worst with 1.177mg/cm² RMSE. In contrary, ARDMatern5/2 kernel-based GPR results in the longest training time of 14.487s (6.9% increase) but its RMSE value is the lowest with 1.084 mg/cm² (by decreasing 7.9%). However, all training time are within 14.5s, which implies that the computational efforts of four ARD kernels are acceptable. In conclusion, through using all feature variables as the input items for ARD kernel-based GPR, expected accuracy can be achieved for the prediction of battery electrode mass load.

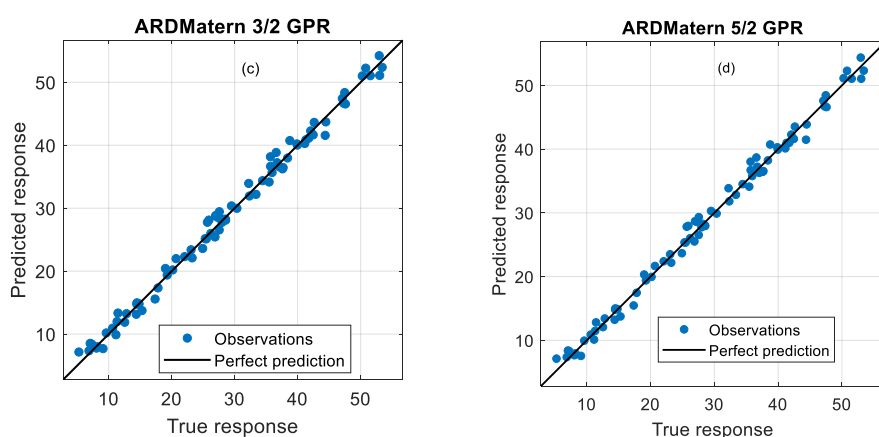
Table 2. Performance metrics for regressions through using all feature items

Kernel types	ARDEX	ARDSE	ARDMatern3/2	ARDMatern5/2
Training time [s]	13.547	13.687	14.154	14.487
MAE [mg/cm ²]	0.946	0.913	0.911	0.875
RMSE [mg/cm ²]	1.177	1.126	1.124	1.084

1



2



3

4 **Fig. 4.** Predicted versus actual plots through using all feature items: (a) ARDEX kernel, (b) ARDSE kernel, (c) ARDMatern3/2
 5 kernel, (d) ARDMatern5/2 kernel.

6 To further reflect the deviations of regression results, the predicted versus actual plots (PVAPs) for all ARD
 7 kernel-based GPRs are shown in Fig. 4. It should be known that in the PVAPs, for the observations on the left or
 8 right of plots, the furthest from the average value would produce the most leverages and effectively pull the
 9 prediction line toward that observation. For a good regression model, the observations should cluster around the
 10 perfect prediction line. According to Fig. 4, all observations are clustered around the perfect prediction lines
 11 without large outliers, indicating that the ARD kernel-based GPRs are capable of achieving satisfactory regression
 12 results with a few deviations for the all feature case.

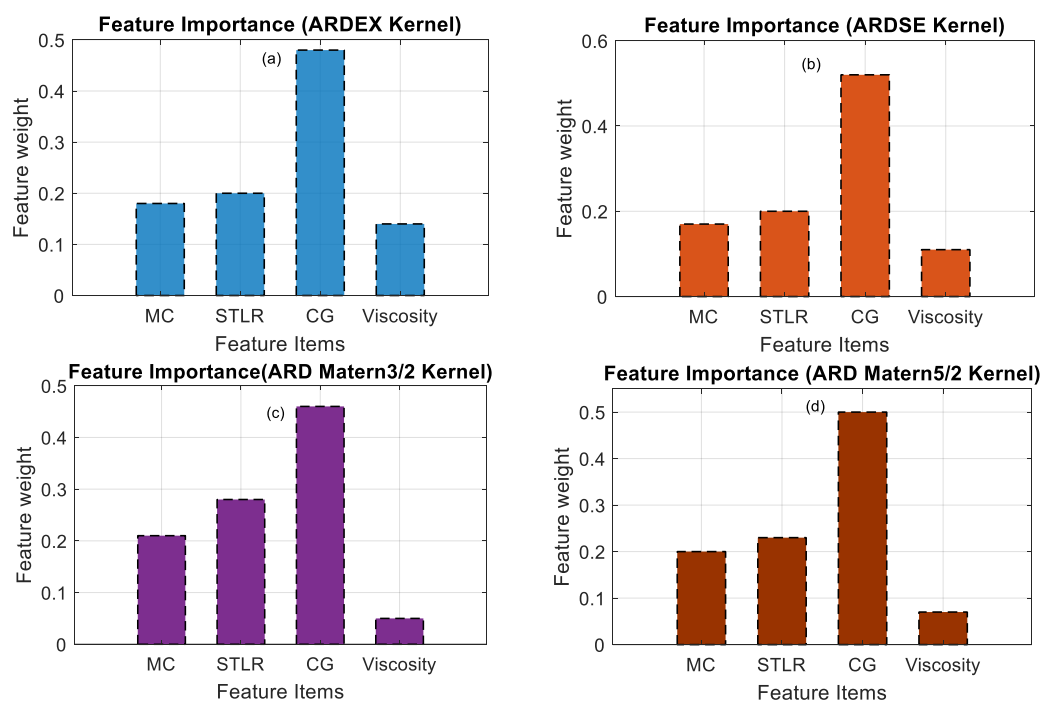


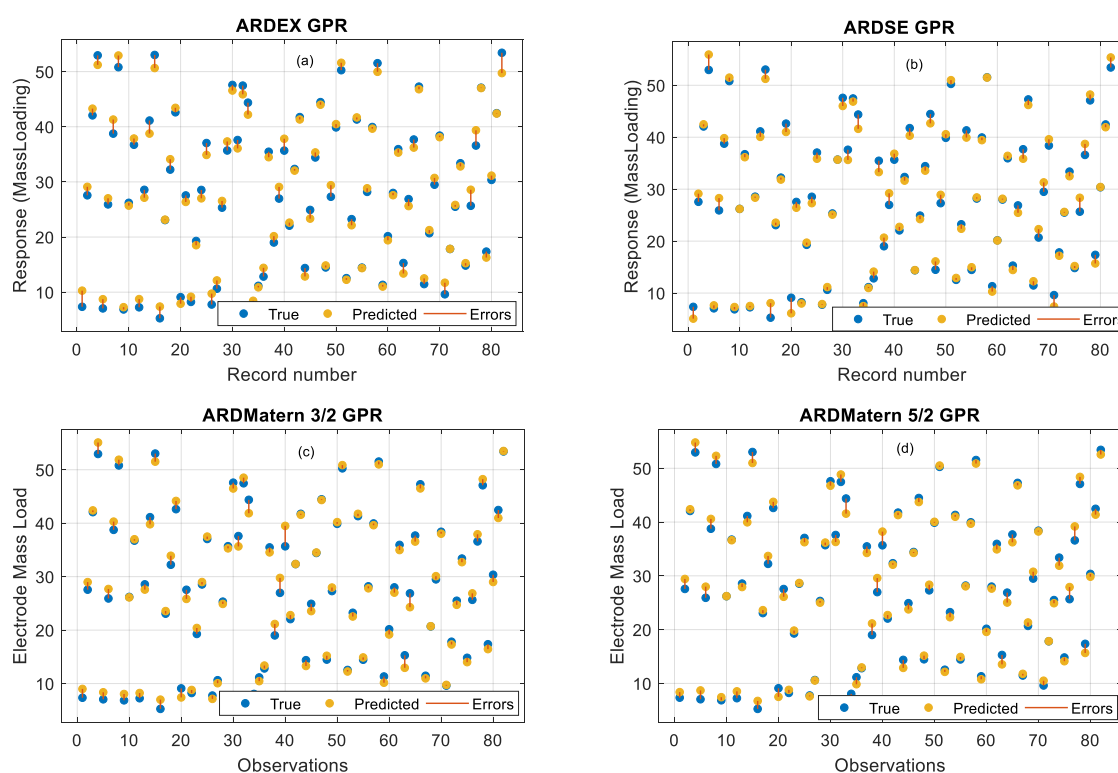
Fig. 5. Obtained feature weights through using various ARD kernels: (a) ARDEX kernel, (b) ARDSE kernel, (c) ARDMatern3/2 kernel, (d) ARDMatern5/2 kernel.

Next, according to the well-tuned GPR models, the normalized feature weights from hyper-parameters of all four ARD kernels are plotted in Fig. 5. Interestingly, although there exists difference among each feature variable, the trend of feature weights is similar for all ARD kernels. Specifically, CG provides the largest feature weight, which is nearly twice as large as the STLR. In contrary, viscosity presents the smallest feature weight (nearly five times less than the CG). The feature weights of STLR are all a slightly larger than those of MC for these ARD kernel cases. This finding signifies that among these four feature variables, CG is the most important one and must be selected for electrode mass load prediction. STLR and MC are the second and third important feature items. In contrast, viscosity makes the least contribution to predicting the battery electrode mass load.

4.2 Case study 2: reduced features

According to the above case study, the weights of all these four feature items are quantified from the hyper-parameters within ARD kernel. Then the importance of these feature variables can be successfully ranked. In accordance with the analysis in Section 4.1, reduced feature tests accounting for less features are carried out in this section to further evaluate the effectiveness of feature ranking. Specifically, the most important three feature variables including CG, STLR and MC are utilised as the input items to evaluate the performance of all ARD

1 kernel-based GPRs again with four-fold cross-validation. As the number of feature items in our study is limited
 2 as four, removing the least important feature item is enough to evaluate the sensitivity analysis of feature variables
 3 in such cases (Zheng and Casari, 2018). When more data of feature variables from battery production chain are
 4 collected to generate a larger feature pool, a solution by setting the threshold for eliminating the particular feature
 5 variables with lower quantified weights can be utilised due to its flexibility. The regression results through using
 6 these reduced feature items and the corresponding performance indicators are presented in Fig. 6 and Table 3,
 7 respectively.



10 **Fig. 6.** Regression results through using reduced feature items for battery electrode mass load predictions: (a) ARDEX kernel,
 11 (b) ARDSE kernel, (c) ARDMatern3/2 kernel, (d) ARDMatern5/2 kernel.

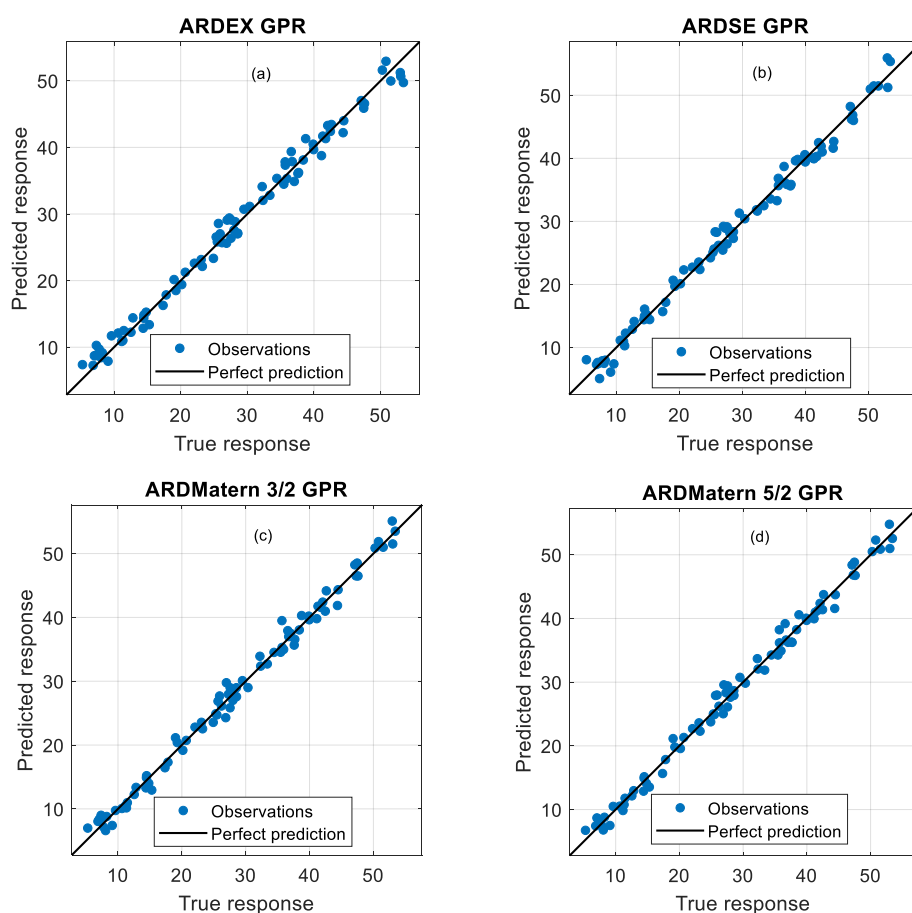
12 **Table 3.** Performance metrics for regressions through using reduced feature items

Kernel types	ARDEX	ARDSE	ARDMatern3/2	ARDMatern5/2
Training time [s]	11.237	11.632	12.986	13.124
MAE [mg/cm ²]	1.197	1.066	0.997	0.985
RMSE [mg/cm ²]	1.433	1.324	1.222	1.204

13

1 It can be noticed that removing one feature item (viscosity) contributes to reducing the training time of all ARD
 2 kernel cases. The maximum training time is 13.124 s for ARDMatern5/2 kernel, which is 9.4% less than its
 3 counterpart with full feature. As observed from Fig. 6, although there exist a few more obvious mismatched
 4 observations, most observations can be still well predicted by the ARD kernel-based GPRs. Quantitatively, the
 5 worst regression performance is observed from ARDEX, with 1.433mg/cm² RMSE (17.7% increase in
 6 comparison with that of all feature case). The ARDMatern kernels still achieve the best regression performance,
 7 which are 1.222mg/cm² RMSE for ARDMatern3/2 (8.7% increase) and 1.204mg/cm² RMSE (9.9% increase) for
 8 ARDMatern5/2, respectively. These results imply that the GPR with ARDMatern kernels provide better accuracy
 9 for electrode mass load prediction in both all feature case and reduced feature case.

10



11

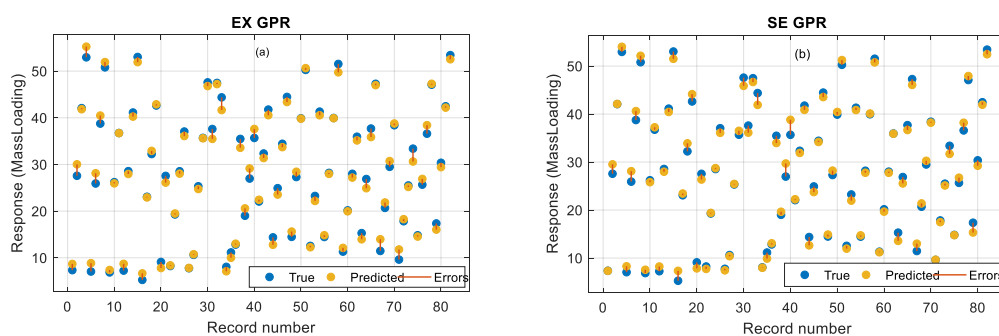
12 **Fig. 7.** Predicted versus actual plots through using reduced feature items: (a) ARDEX kernel, (b) ARDSE kernel, (c)
 13 ARDMatern3/2 kernel, (d) ARDMatern5/2 kernel.

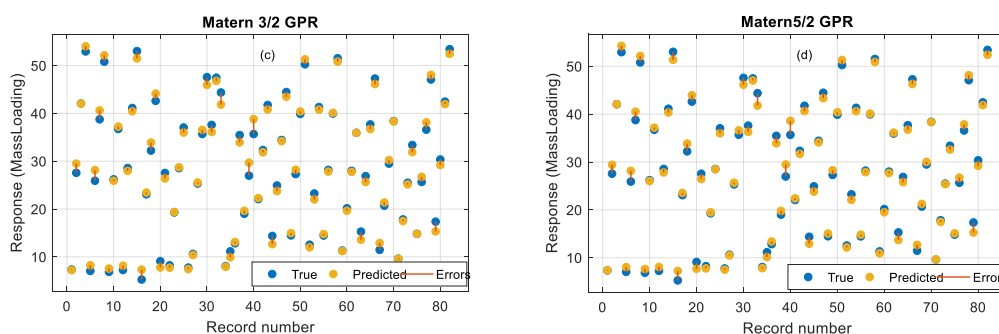
14 To reflect the deviations of these regression results, the PVAPs using GPRs with reduced feature variables are
 15 shown in Fig. 7. In comparison with the PVAPs using all features, the deviations of observations in the reduced

1 feature case spread over a wide uncertain region. However, all observations are still dispersed around the perfect
2 prediction lines closely, which means that none obvious prediction outliers are generated in all ARD kernel cases.
3 In summary, after removing the viscosity item with the lowest feature weight, the ARD-kernel based GPRs can
4 still provide satisfactory regression results for electrode mass load. These results imply that the feature importance
5 weights can be successfully quantified by the designed ARD kernel. For the battery production chain that contains
6 numerous feature variables, the proposed ARD kernel-based GPR is able to not only reduce the feature dimension
7 but also guarantee the performance of electrode property regression, further helping to promote the efficiencies.

8 In our study, following the same flow in many feature engineering applications (Dong and Liu, 2018; Zheng and
9 Casari, 2018), the ARD-kernel based GPR with all features is first utilised to get importance ranking of these
10 features and then the reduced features GPR is adopted for further evaluating the correctness of selected features.
11 Due to the number of features is four, we only remove a feature variable with lower importance weight in the
12 reduced feature GPR case, further resulting the training time is not highly reduced. As battery production chain is
13 a highly-complicated process with numerous feature variables in total, monitoring all feature variables and using
14 full features to build a model is time-consuming and unrealistic. In light of this, when more feature data within
15 battery production chain are available, the advantages of using a reduced features GPR would become more
16 obvious as it could help to remove more irrelevant feature items and reduce the training time without sacrificing
17 much accuracy.

18 4.3 Performance comparison with conventional kernels





1
2 **Fig. 8.** Comparison results through using conventional kernels with all feature items: (a) EX kernel, (b) SE kernel, (c) Matern3/2
3 kernel, (d) Matern5/2 kernel.

4 **Table 4.** Performance metrics for regressions through using all feature items

Kernel types	EX	SE	Matern3/2	Matern5/2
Training time [s]	13.323	13.586	13.964	13.959
MAE [mg/cm ²]	0.994	0.983	0.958	0.907
RMSE [mg/cm ²]	1.317	1.292	1.184	1.151

5
6 To further reflect the prediction performance of ARD kernels, four GPR models with the related conventional
7 kernels of EX, SE, Matern3/2 and Matern5/2 are adopted as the benchmarks for comparison purpose. According
8 to the specific forms as illustrated in Eqs. (8), (9), (10) and (11), these convention kernels without ARD structure
9 cannot directly quantify the feature importance as the hyper-parameters of all four feature items within the kernel
10 are same. Fig. 8 and Table 4 illustrate the regression results and corresponding performance metrics of using all
11 four feature items as inputs to the conventional kernel-based GPRs after four-folds cross-validation. It can be seen
12 that EX kernel shows the worst results, while Matern3/2 and Matern5/2 provide better regression results. Here the
13 RMSEs of all conventional kernels are a slightly worse than the related ARD kernels (5% increase). Therefore,
14 apart from the superiority in terms of interpretability of feature importance, ARD kernel-based GPRs also present
15 competent performance in the prediction of battery electrode mass load.

16 **4.4 Implications for theory and practice on battery production**

17 The ARD kernels-based GPR machine learning framework proposed in this study has extensive application
18 prospects for the predictions of battery product properties and the sensitivity analysis of various feature variables
19 in battery production application. For instance, the properties of manufactured electrode play a key role in

1 determining the battery final performance (energy or power densities, maximal capacity and service life), which
2 must be carefully predicted and managed. Besides, the battery production chain contains many intermediate stages
3 such as mixing, coating, drying and calendaring. All these stages cover multiple disciplines such as mechanical,
4 chemical and electrical engineering, making the traditional sensitivity analysis by trial and error way is
5 significantly time-consuming. Another complication is that battery production chain has numerous strong-coupled
6 feature variables in total, monitoring all feature variables and using full features to build a model is inefficient and
7 unrealistic. In light of this, this paper proposes the idea to simultaneously predict battery electrode property and
8 analyse feature importance through machine learning approach. When more feature data within battery production
9 chain are available, the proposed framework could help to remove more irrelevant feature items and reduce the
10 training time without sacrificing much accuracy. The battery manufacturer can utilise the feature importance
11 information and property prediction results from our model to redesign the monitor variables and readjust the
12 process parameters to improve the manufacturing performance, so as to ensure the effectiveness of monitored
13 feature variables and the satisfactory qualities of cleaner battery production.

14 **5. Conclusion**

15 As the electrode production plays a key role in affecting the results and performance for cleaner battery production,
16 the efficient electrode mass load prediction and feature selection of battery intermediate products are presented in
17 this study. An advanced machine learning approach, based on the GPR technology with various ARD kernels, is
18 developed to effectively predict the battery electrode mass load. Meanwhile, the importance weights of four
19 feature variables of interest in the mixing and coating steps are also directly quantified through analysing the
20 hyper-parameters within ARD kernels. According to the quantitative comparison and sensitivity analysis of results,
21 the main conclusions can be summarized as:

22 1) The ARD kernel-based GPRs are capable of not only predicting electrode mass load (here the RMSEs are at
23 least 5% better than those from conventional kernel-based GPRs) but also well quantifying the importance weights
24 for all four feature variables (MC, STLR, CG and viscosity). The obtained importance ranking can well benefit
25 the feature selection and model dimension reduction for efficient battery production.

1 2) Among four ARD kernel functions, the ARDMatern5/2 kernel achieves the best regression performance for
2 the cases of either using all feature items (at least 4% improved) or reduced feature items as inputs (at least 2%
3 improved), making it more suitable for property prognostics of battery electrode production.

4 3) CG from coating stage is most crucial for electrode mass load regression among four feature variables of interest.
5 Here the quantified importance value of CG is twice more than others. Therefore, CG should be well monitored
6 and controlled to obtain electrode product with reliable performance.

7 4) On the contrary, viscosity from mixing stage makes the least contribution to the electrode mass load regression
8 (9.9% RMSE increases). To further improve the performance of electrode mass load prognostics in battery
9 production, the battery manufacturer should pay more attention to MC and STLR when operating the mixing stage.

10 This is the first known application by deriving ARD kernel-based GPR framework to directly and simultaneously
11 predict battery electrode property as well as analyse feature importance. As the designed machine learning
12 framework in our study belongs to a data-driven approach with the superiority in terms of accuracy and flexibility,
13 it can be conveniently extended to analyse other variables within the battery production chain when the
14 corresponding data are available. Our future work would focus on designing extra experiments to generate more
15 available data from other battery production process (i.e., mixing, drying and calendaring), and then to conduct
16 reliable sensitivity analysis and feature selection for more variables within battery production chain, further
17 benefitting the cleaner battery production and optimal energy storage system design.

18 **Acknowledgements**

19 This work is supported by the EPSRC under grant EP/R030243/1, the National Key Research and Development
20 Project under Grant 2018YFB 1700503, and the Natural Science Foundation of Guangdong under Grant No.
21 2018A 030310671. The authors would like to thank professor Jihong Wang from School of Engineering,
22 University of Warwick for fruitful discussions and proofreading.

23 **Reference**

24 Chouchane, M., Rucci, A., Lombardo, T., Ngandjong, A.C., Franco, A.A., 2019. Lithium ion battery
25 electrodes predicted from manufacturing simulations: Assessing the impact of the carbon-binder
26 spatial location on the electrochemical performance. JPS 444, 227285.
27 <https://doi.org/10.1016/j.jpowsour.2019.227285>

- 1 Cunha, R.P., Lombardo, T., Primo, E.N., Franco, A.A., 2020. Artificial Intelligence Investigation of NMC
2 Cathode Manufacturing Parameters Interdependencies. *Batteries & Supercaps* 3(1), 60-67.
3 <https://doi.org/10.1002/batt.201900135>
- 4 Dahodwalla, H., Herat, S., 2000. Cleaner production options for lead-acid battery manufacturing
5 industry. *J. Clean. Prod.* 8(2), 133-142. [https://doi.org/10.1016/S0959-6526\(99\)00314-5](https://doi.org/10.1016/S0959-6526(99)00314-5)
- 6 Dong, G., Liu, H., 2018. *Feature Engineering for Machine Learning and Data Analytics*. CRC Press.
- 7 Günther, T., Schreiner, D., Metkar, A., Meyer, C., Kwade, A., Reinhart, G., 2020. Classification of
8 Calendering - Induced Electrode Defects and Their Influence on Subsequent Processes of
9 Lithium - Ion Battery Production. *Energy Technol.* 8(2), 1900026.
10 <https://doi.org/10.1002/ente.201900026>
- 11 He, H., Tian, S., Tarroja, B., Ogunseitani, O.A., Samuelsen, S., Schoenung, J.M., 2020. Flow battery
12 production: Materials selection and environmental impact. *J. Clean. Prod.* 269, 121740.
13 <https://doi.org/10.1016/j.jclepro.2020.121740>
- 14 Hoffmann, L., Grathwol, J.-K., Haselrieder, W., Leithoff, R., Jansen, T., Dilger, K., Dröder, K., Kwade, A.,
15 Kurrat, M., 2019. Capacity Distribution of Large Lithium-Ion Battery Pouch Cells in Context with
16 Pilot Production Processes. *Energy Technol.* 8. <https://doi.org/10.1002/ente.201900196>
- 17 Jacobs, J.P., 2012. Bayesian Support Vector Regression With Automatic Relevance Determination
18 Kernel for Modeling of Antenna Input Characteristics. *IEEE Trans. Antennas Propag.* 60(4), 2114-
19 2118. <https://doi.org/10.1109/TAP.2012.2186252>
- 20 Knoche, T., Surek, F., Reinhart, G., 2016. A Process Model for the Electrolyte Filling of Lithium-ion
21 Batteries. *Procedia CIRP* 41, 405-410. <https://doi.org/10.1016/j.procir.2015.12.044>
- 22 Kwade, A., Haselrieder, W., Leithoff, R., Modlinger, A., Dietrich, F., Droeder, K., 2018. Current status
23 and challenges for automotive battery production technologies. *Nat. Energy* 3(4), 290-300.
24 <https://doi.org/10.1038/s41560-018-0130-3>
- 25 Lee, S.S., Kim, T.H., Hu, S.J., Cai, W.W., Abell, J.A., 2010. Joining Technologies for Automotive Lithium-
26 Ion Battery Manufacturing: A Review. *ASME 2010 International Manufacturing Science and
27 Engineering Conference*, Volume 1, 541-549. <https://doi.org/10.1115/MSEC2010-34168>
- 28 Li, Y., Liu, K., Foley, A.M., Zülke, A., Bercebar, M., Nanini-Maury, E., Van Mierlo, J., Hoster, H.E., 2019.
29 Data-driven health estimation and lifetime prediction of lithium-ion batteries: A review. *Renew.
30 Sust. Energ. Rev.* 113, 109254. <https://doi.org/10.1016/j.rser.2019.109254>
- 31 Lipu, M.S.H., Hannan, M.A., Hussain, A., Hoque, M.M., Ker, P.J., Saad, M.H.M., Ayob, A., 2018. A review
32 of state of health and remaining useful life estimation methods for lithium-ion battery in electric
33 vehicles: Challenges and recommendations. *J. Clean. Prod.* 205, 115-133.
34 <https://doi.org/10.1016/j.jclepro.2018.09.065>
- 35 Liu, C., Lin, J., Cao, H., Zhang, Y., Sun, Z., 2019. Recycling of spent lithium-ion batteries in view of lithium
36 recovery: A critical review. *J. Clean. Prod.* 228, 801-813.
37 <https://doi.org/10.1016/j.jclepro.2019.04.304>
- 38 Liu, K., Hu, X., Wei, Z., Li, Y., Jiang, Y., 2019. Modified Gaussian Process Regression Models for Cyclic
39 Capacity Prediction of Lithium-Ion Batteries. *IEEE Trans. Transp. Electrification* 5(4), 1225-1236.
40 <https://doi.org/10.1109/TTE.2019.2944802>
- 41 Liu, K., Li, Y., Hu, X., Lucu, M., Widanalage, D., 2019. Gaussian Process Regression with Automatic
42 Relevance Determination Kernel for Calendar Aging Prediction of Lithium-ion Batteries. *IEEE
43 Transactions on Industrial Informatics* PP, 1-1. <https://doi.org/10.1109/TII.2019.2941747>
- 44 Liu, K., Shang, Y., Ouyang, Q., Widanage, W.D., 2020. A Data-driven Approach with Uncertainty
45 Quantification for Predicting Future Capacities and Remaining Useful Life of Lithium-ion Battery.
46 *ITIE*, 1-1. <https://doi.org/10.1109/TIE.2020.2973876>

- 1 Liu, K., Zou, C., Li, K., Wik, T., 2018. Charging Pattern Optimization for Lithium-Ion Batteries With an
2 Electrothermal-Aging Model. *IEEE Transactions on Industrial Informatics* 14(12), 5463-5474.
3 <https://doi.org/10.1109/TII.2018.2866493>
- 4 Maia, L.K.K., Drünert, L., La Mantia, F., Zondervan, E., 2019. Expanding the lifetime of Li-ion batteries
5 through optimization of charging profiles. *J. Clean. Prod.* 225, 928-938.
6 <https://doi.org/10.1016/j.jclepro.2019.04.031>
- 7 Meng, J., Stroe, D., Ricco, M., Luo, G., Swierczynski, M., Teodorescu, R., 2019. A Novel Multiple
8 Correction Approach for Fast Open Circuit Voltage Prediction of Lithium-Ion Battery. *ITEnC* 34(2),
9 1115-1123. <https://doi.org/10.1109/TEC.2018.2880561>
- 10 Ouyang, Q., Wang, Z., Liu, K., Xu, G., Li, Y., 2020. Optimal Charging Control for Lithium-Ion Battery
11 Packs: A Distributed Average Tracking Approach. *IEEE Transactions on Industrial Informatics* 16(5),
12 3430-3438. <https://doi.org/10.1109/TII.2019.2951060>
- 13 Pan, Y., Feng, X., Zhang, M., Han, X., Lu, L., Ouyang, M., 2020. Internal short circuit detection for
14 lithium-ion battery pack with parallel-series hybrid connections. *J. Clean. Prod.* 255, 120277.
15 <https://doi.org/10.1016/j.jclepro.2020.120277>
- 16 Pang, Y., Cao, Y., Chu, Y., Liu, M., Snyder, K., MacKenzie, D., Cao, C., 2019. Additive Manufacturing of
17 Batteries. *Adv. Funct. Mater.*, 1906244. <https://doi.org/10.1002/adfm.201906244>
- 18 Rasmussen, C.E., Williams, C.K.I., 2006. *Gaussian Processes for Machine Learning*. University Press
19 Group Limited.
- 20 Richardson, R.R., Birkel, C.R., Osborne, M.A., Howey, D.A., 2019. Gaussian Process Regression for In Situ
21 Capacity Estimation of Lithium-Ion Batteries. *IEEE Transactions on Industrial Informatics* 15(1),
22 127-138. <https://doi.org/10.1109/TII.2018.2794997>
- 23 Saw, L.H., Ye, Y., Tay, A.A.O., 2016. Integration issues of lithium-ion battery into electric vehicles
24 battery pack. *J. Clean. Prod.* 113, 1032-1045. <https://doi.org/10.1016/j.jclepro.2015.11.011>
- 25 Schnell, J., Nentwich, C., Endres, F., Kollenda, A., Distel, F., Knoche, T., Reinhart, G., 2019. Data mining
26 in lithium-ion battery cell production. *JPS* 413, 360-366.
27 <https://doi.org/10.1016/j.jpowsour.2018.12.062>
- 28 Schnell, J., Reinhart, G., 2016. Quality Management for Battery Production: A Quality Gate Concept.
29 *Procedia CIRP* 57, 568-573. <https://doi.org/10.1016/j.procir.2016.11.098>
- 30 Schünemann, J.-H., Dreger, H., Bockholt, H., Kwade, A., 2016. Smart Electrode Processing for Battery
31 Cost Reduction. *ECS Transactions* 73, 153-159. <https://doi.org/10.1149/07301.0153ecst>
- 32 Shang, Y., Liu, K., Cui, N., Wang, N., Li, K., Zhang, C., 2019. A Compact Resonant Switched-Capacitor
33 Heater for Lithium-Ion Battery Self-Heating at Low Temperatures. *ITPE PP*, 1-1.
34 <https://doi.org/10.1109/TPEL.2019.2954703>
- 35 Tagade, P., Hariharan, K.S., Ramachandran, S., Khandelwal, A., Naha, A., Kolake, S.M., Han, S.H., 2020.
36 Deep Gaussian process regression for lithium-ion battery health prognosis and degradation mode
37 diagnosis. *JPS* 445, 227281. <https://doi.org/10.1016/j.jpowsour.2019.227281>
- 38 Tang, X., Liu, K., Wang, X., Liu, B., Gao, F., Widanage, W.D., 2019. Real-time aging trajectory prediction
39 using a base model-oriented gradient-correction particle filter for Lithium-ion batteries. *JPS* 440,
40 227118. <https://doi.org/10.1016/j.jpowsour.2019.227118>
- 41 Thiede, S., Turetskyy, A., Kwade, A., Kara, S., Herrmann, C., 2019. Data mining in battery production
42 chains towards multi-criterial quality prediction. *CIRP Annals* 68.
43 <https://doi.org/10.1016/j.cirp.2019.04.066>
- 44 Tian, H., Qin, P., Li, K., Zhao, Z., 2020. A review of the state of health for lithium-ion batteries: Research
45 status and suggestions. *J. Clean. Prod.* 261, 120813.
46 <https://doi.org/10.1016/j.jclepro.2020.120813>

- 1 Turetskyy, A., Thiede, S., Thomitzek, M., von Drachenfels, N., Pape, T., Herrmann, C., 2019. Toward
2 Data - Driven Applications in Lithium - Ion Battery Cell Manufacturing. Energy Technol.
3 <https://doi.org/10.1002/ente.201900136>
- 4 Wanner, J., Weeber, M., Birke, K.P., Sauer, A., 2019. Quality Modelling in Battery Cell Manufacturing
5 Using Soft Sensing and Sensor Fusion - A Review. 2019 9th International Electric Drives
6 Production Conference (EDPC), 1-9. <https://doi.org/10.1109/EDPC48408.2019.9011847>
- 7 Wei, Z., Zhao, J., Xiong, R., Dong, G., Pou, J., Tseng, K.J., 2019. Online Estimation of Power Capacity
8 With Noise Effect Attenuation for Lithium-Ion Battery. ITIE 66(7), 5724-5735.
9 <https://doi.org/10.1109/TIE.2018.2878122>
- 10 Xiong, R., Chen, H., Wang, C., Sun, F., 2018. Towards a smarter hybrid energy storage system based on
11 battery and ultracapacitor - A critical review on topology and energy management. J. Clean. Prod.
12 202, 1228-1240. <https://doi.org/10.1016/j.jclepro.2018.08.134>
- 13 Yang, D., Zhang, X., Pan, R., Wang, Y., Chen, Z., 2018. A novel Gaussian process regression model for
14 state-of-health estimation of lithium-ion battery using charging curve. JPS 384, 387-395.
15 <https://doi.org/10.1016/j.jpowsour.2018.03.015>
- 16 Yang, R., Xiong, R., He, H., Chen, Z., 2018. A fractional-order model-based battery external short circuit
17 fault diagnosis approach for all-climate electric vehicles application. J. Clean. Prod. 187, 950-959.
18 <https://doi.org/10.1016/j.jclepro.2018.03.259>
- 19 Zhang, Y., Tang, Q., Zhang, Y., Wang, J., Stimming, U., Lee, A.A., 2020. Identifying degradation patterns
20 of lithium ion batteries from impedance spectroscopy using machine learning. Nat. Commun. 11(1),
21 1706. <https://doi.org/10.1038/s41467-020-15235-7>
- 22 Zhang, Y., Xiong, R., He, H., Pecht, M., 2019. Validation and verification of a hybrid method for
23 remaining useful life prediction of lithium-ion batteries. J. Clean. Prod. 212, 240-249.
24 <https://doi.org/10.1016/j.jclepro.2018.12.041>
- 25 Zhao, J., Chen, L., Pedrycz, W., Wang, W., 2019. Variational Inference-Based Automatic Relevance
26 Determination Kernel for Embedded Feature Selection of Noisy Industrial Data. ITIE 66(1), 416-428.
27 <https://doi.org/10.1109/TIE.2018.2815997>
- 28 Zheng, A., Casari, A., 2018. Feature Engineering for Machine Learning: Principles and Techniques for
29 Data Scientists. O'Reilly Media.
- 30 Zhou, Z., Duan, B., Kang, Y., Shang, Y., Cui, N., Chang, L., Zhang, C., 2020. An efficient screening method
31 for retired lithium-ion batteries based on support vector machine. J. Clean. Prod. 267, 121882.
32 <https://doi.org/10.1016/j.jclepro.2020.121882>
- 33 Zhou, Z., Kang, Y., Shang, Y., Cui, N., Zhang, C., Duan, B., 2019. Peak power prediction for series-
34 connected LiNCM battery pack based on representative cells. J. Clean. Prod. 230, 1061-1073.
35 <https://doi.org/10.1016/j.jclepro.2019.05.144>